

## Production and Characterization of Rice Husk Biochar and Kenaf Biochar for Value-Added Biochar Replacement for Potential Materials Adsorption

Anwar Ameen Hezam Saeed<sup>1</sup>, Noorfidza Yub Harun<sup>1\*</sup>, Suriati Sufian<sup>1</sup>, Haruna Kolawole Afolabi<sup>1</sup>, Ebrahim Hamid Hussein Al-Qadami<sup>2</sup>, Farah Amelia Shahirah Roslan<sup>1</sup>, Syahirah Abdul Rahim<sup>1</sup>, A.A.S. Ghaleb<sup>2</sup>

<sup>1</sup> Department of Chemical Engineering, Universiti Teknologi PETRONAS, Bandar Seri Iskandar, Perak, Malaysia

<sup>2</sup> Department of Civil and Environmental Engineering, Universiti Teknologi PETRONAS, Seri Iskandar, Perak Darul Ridzuan, Malaysia

\* Corresponding author's email: noorfidza.yub@utp.edu.my

### ABSTRACT

Two raw biomass materials from different sources were investigated: aluminosilicate obtained from rice husk and agricultural lignocellulosic waste from kenaf fiber. The properties of the optimal mixing ratio of biochar were investigated by using proximate analysis, ultimate analysis, thermogravimetric analysis, surface area and pore volume determination, Fourier Transform Infrared Spectroscopy analysis, X-ray diffraction, and Scanning Electron Microscopy. According to the proximate analysis, the ash content is increasing while the moisture content fixed carbon and volatile matter decrease. On the basis of the BET characterization finding, the surface area is increased proportionally to the increasing mixing ratio RHB: KFB (0.8:0.2, 0.5:0.5, 0.2:0.8). The SEM images showed that both biochars are suitable sources of blending because of the differences and the availability of good adsorbents. This study indicated that RHB and KFB as pure biochar have a great potential to be applied as adsorbents. However, blending is not giving the desired result to be used as an adsorbent.

**Keywords:** biochar, biomass, adsorption, blending, kenaf fiber, rice husk, pyrolysis

### INTRODUCTION

Most industrial wastewater is highly persistent; otherwise, it will turn into a recalcitrant form. Water pollution posed different hazards to humans, animals, and plants on Earth. The water pollution is included in many classifications like organic pollution such as phenol, ammonia, dyes, and other aromatics substances found in industries. Furthermore, heavy metals such as copper, cadmium, arsenic, chromium, mercury, zinc, and other metals from the metal finishing industries are released during electroplating and coating to wastewater. Due to the chronic consequences of heavy metals to a human being, the removal treatment for those dangerous heavy metals must be performed before discharging. Many advanced

technologies are applied for heavy metal removal such as chemical precipitation, flotation, ion exchange, coagulation, flocculation, membrane filtration, and adsorption (Renu, Agarwal, and Singh 2017; Saeed 2020).

Among all the methods mentioned above, the adsorption method is considered as an additive, efficient technology that can be used to remove heavy metals from wastewater and provide a quantitative amount of treated wastewater (Ardejani et al. 2007). Various adsorbents, like activated carbon, activated biochar, are the most employed method. Malaysia is one of those countries which are rich in agricultural waste such as rice husk, empty fruits bunch, coconut shell, and kenaf fiber. Malaysia generates more than 2 million tons of agricultural waste annually which is disposed

of or consumed in an open dump that causes numerous environmental problems, such as contamination of groundwater and air (Mubarak et al. 2014). The Malaysian agricultural wastes were developed into biochar and composite biochar by using many biochar production technologies such as pyrolysis, hydrothermal and other technologies (Chan et al. 2008; Harun et al. 2019). Pyrolysis is the most common and successful technology is of biochar production, which can also be used as a heavy metal removal adsorbent (Liu and Zhang 2009). The result of pyrolysis is the carbonization of biomass or biochar to comply with an ancient philosophy. The biochar, a kind of porous carbon like activated carbon, has several agronomic advantages and environmental benefits, such as soil enhancement, surface contamination adsorption, as well as remediation of inorganic and organic contaminants in soils (Saeed et al. 2018).

Rice husk is one of the major agricultural by-products produced during the paddy rice distillation. Globally, 20 percent of the 500 billion tons of rice produced is projected to be rice husks. The handling of rice husks poses significant environmental risks because the silicon material is immune to natural decomposition. One of the main parameters influencing the properties of rice husk ash combined with other materials is its method of combustion and processing. Kenaf is agricultural biomass used with the acid chemical activating agent to generate low-cost activated carbon. Kenaf has two kinds of fibers to be examined for the AC output. Long fibers account for about 30% of the total plant volume, while short fibers account for the remaining 70%.

## MATERIALS AND METHODS

### Materials

The two kinds of agricultural waste selected as precursors for biochar preparation are rice husk and kenaf fiber. Both agricultural wastes are local; the rice husk is brought from the rice mill (Bota), while the kenaf fiber gets shipped from Pahang. The samples were washed to remove gravel, sand, and unwanted material from it. Then, they were dried in an open atmosphere for two days and dried in an oven at 105 °C for 24 hours. The samples were subjected to grinding, sieving to one form of size ranging from 500–1,000 µm. It was then placed in an airtight

container at room temperature before characterizations and experiments.

A horizontal tube furnace for slow pyrolysis was developed to pyrolyze the feedstock. The dried biomass was placed in Ceramic Crucible Boat. Pyrolysis was performed at a constant temperature of 500 °C for 60 minutes. The nitrogen as the carrier gas was fed at flowrate 100 cm<sup>3</sup>/min into the reactor. Biochar was collected and weighed after cooling.

Each biochar underwent the washing process using distilled water until neutral pH was achieved. Then, 5 samples were prepared at the blended ratio RHB to KFB amounting to 1.0:0.0, 0.2:0.8, 0.5:0.5, 0.8:0.2 and 0.0:1.0 by wt.%.

Copper (II) stock solution was prepared by dissolving Copper (II) nitrate trihydrate (Cu(NO<sub>3</sub>)<sub>2</sub>·3H<sub>2</sub>O) into a 1000 mg/L solution and then diluting the solution to the appropriate specific solutions. Atomic absorption spectrometry was used to determine the initial concentrations and the residual concentration. The pH of the solution was measured with a pH meter and monitored by using HCl and NaOH.

The batch adsorption experiments were conducted using various biochar as adsorbents. A 30-ppm synthetic copper (II) solution with a fixed concentration of metal ion was put in such a sequence of 250 mL of Erlenmeyer flasks. The flask was shaken at 200 rpm using an orbital shaker at room temperature (25±1 °C) for one hour. The mixture was extracted by using Whatman's glass microfiber filter paper at the later part of the specified stirring period. The analysis of residual copper (II) content in a diluted solution was performed using inductively coupled plasma emission spectrometry. All the studies were conducted using the same parameters, pH at 6, rotation time 60 min, and shaking rate (200 rpm). The removal efficiency of biochar adsorbent was calculated by using Eq. 1:

$$\text{Removal Efficiency} = \frac{C_i - C_e}{C_i} \cdot 100, \% \quad (1)$$

where:  $C_i$  is referred to as the initial concentration while the  $C_e$  is referred to as residual concentration (mg/l) of the solution.

### Characterization of materials

The biomass used for this analysis was classified according to its chemical, structural, and texture characteristics. The ASTM standard method (ASTM E870-829) iwass used to

characterize the sample for the approximate analysis and ultimate analysis.

The ultimate analysis was carried out to evaluate the biomass and biochar elements. The simple model CHNS Elemental Analyser was used, according to ASTM D5373-02. The tests were conducted in compliance with ASTM Code D5142-02a which involved the study of the ash content, fixed carbon content, moisture content, and volatile material.

The mathematical method used comprises the simple equations that control the oxygen content determination and biomass calorific value. Through 100% extracting the volume of (C, H, N, S, and Ash) wt.% dry basis, the oxygen content was obtained as shown in Eq. 2 and Eq. 3:

$$F.C = 100 - (M.C + A.C + V.M) \text{ (wt.\%)} \quad (2)$$

$$O = 100 - (M.C + A.C + C + H + N) \text{ (wt.\%)} \quad (3)$$

where: M.C, A.C, V.M, F.C, O, C, H, and N, in Eq. 2 and Eq. 3 represent the moisture content, ash content, volatile matter, fixed carbon, oxygen, carbon, hydrogen, and nitrogen, respectively.

Functional groups have structural units within organic compounds identified by different atom and bond arrangements that give each sample their own merits. FTIR spectroscopy, was performed using Fourier transform infrared spectroscopy to determine the functional groups attached to the surface of raw biomass and biochar. In addition, it enabled to measure changes in the functional groups of modified and unmodified samples.

The TGA pyrolysis of the biomass samples and biochar samples were carried out under a nitrogen ( $N_2$ ) atmosphere at 150 ml/min. A biomass sample between 0.5 and 1.0 mg was pyrolyzed to a maximum temperature of 700 °C. The sample was first heated to 110 °C and held for 30 minutes to remove any moisture. Thereafter, the sample was separately heated at a rate of 20 °C/min until it reached maximum temperature. The experiment was repeated for each biomass. A graph of

mass loss versus temperature and a plot of mass loss versus temperature were plotted to observe the degradation behavior of each type of biomass and biochar.

Surface area, pore diameter, and pore volume were measured by using surface area Analyzer and porosimeter system model Micromeritics ASAP 2020. The surface morphology and elemental qualitative analysis of the samples were carried out using the Scanning Electron Microscopy analyzer.

## RESULTS AND DISCUSSION

### Proximate and ultimate analysis

Proximate analysis was performed to assess the characteristics of the pure biochar, blended biochar, relative to the raw materials. The moisture, volatile matter, ash content, and fixed carbon obtained from this analysis are shown in Table 1. Blending biochar with a ratio of 0.20 to 0.80 rice husk biochar to Kenaf biochar has the highest fixed carbon content moisture compared to the other ratio with 56.9%. The possibility of obtaining stable solid fuel (biochar) increases if the volatile matter of biomass is high (Tan et al. 2015). Table 1, shows that the volatile matter of the kenaf biomass is higher than that of rice husk. These are two properties for the handling of chemicals or waste materials, the volume of volatile matter in biochar and the carbon content of the biochar set. Biochar has low variability and strong carbon content, which allows the biochar the capacity to adsorb toxins or waste particles across pores (Saeed et al. 2018).

The C, H, N, O composition analysis of different kinds of biomass and biochar in Table 2 shows that the rice husk biochar (RHB pure) recorded higher C (56.4%) and H (2.97%) with low N (0.26%) content. The kenaf biochar recorded high N (1.2%) and low carbon content (46.7%). The amount of oxygen was high almost

**Table 1.** Proximate analysis of raw materials and prepared pristine and blended biochar

Proximate (wt.%)	Sample ratio Rice Husk: Kenaf					Sample ratio RHB: KFB				
	1.0:0	0.80:0.20	0.50:0.50	0.20:0.80	0.0:1.0	1.0:0	0.80:0.20	0.50:0.50	0.20:0.80	0.0:1.0
Moisture	9.427	10.1	8.90	9.15	8.35	2.5	2.8	3.2	3.25	3.4
Volatile matter	61.982	59.45	60.1	64.35	67.2	14	15.5	16.1	16.8	17.5
Ash	16.32	15.6	14.9	13.50	13.223	31.6	28	27.5	23	22.7
Fixed carbon	12.27	14.85	16.1	13	11.22	49.5	53.7	53.2	56.95	56.4

in all the biomass and biochar samples which may tell us that the pyrolysis temperature was not enough to break the oxygen bond. The hydrogen-to-carbon (H:C) ratio is commonly used to calculate the degree and maturation of the biochar following its long-term environmental stability. All biochar samples in this study had an H:C ratio of less than 0.080, which indicated that biochar did not alter enough thermochemically (Standards 2012). Typical oxygen to carbon ratios (O:C) are between 0.2 and 0.6, which are called char and the O/C ratio indicates the polarity, and abundance of polar oxygen-containing surface functional groups in biochar. The higher the ratio, the more polar functional groups there are. Moreover, these groups actively take part in the adsorption of heavy metals. This study found that the oxygen to carbon ratios of pure rice husk biochar (RHB) enable considering it as stable biochar.

### FTIR spectra

Figure 1 shows the FTIR spectra of raw rice husk (RRH), raw kenaf (RKF), rice husk biochar (RHB), kenaf fiber biochar (KFB), and composite biochar (RHCK) at a wavelength ranging from 500  $\text{cm}^{-1}$  to 5000  $\text{cm}^{-1}$ . The absorption band at 3400  $\text{cm}^{-1}$  indicates the O-H link and the hydroxyl group of hydrogen bonding in the unpyrolyzed samples. The peaks up and down between the wavelength of 1750  $\text{cm}^{-1}$  to 1350  $\text{cm}^{-1}$  in most of the biochar indicate C=O and C-O stretching, which is notorious with organic ester linkage of hemicellulose and p-coumaric acids of lignin. The spectrums of all RRH and RHB exhibit differences. For instance, the peaks at 1100  $\text{cm}^{-1}$  and 900  $\text{cm}^{-1}$ , which can be ascribed to Si-O and Si-H stretching vibrations appear in RH and RHB, but not the other samples due to the presence of silica content in the rice husk.

### XRD analysis

The X-ray diffraction pattern in a wide-angle region ( $10\text{--}60^\circ$ ) will assess synthetic biochar graphite properties. As can be seen from Figure 2, the crystalline peak observed around the  $2\theta$  scale between  $20^\circ$  and  $22^\circ$  confirms the presence of cellulose which renders crystallinity to the particles. However, peak intensity varies from one sample to another; for example, the peak intensity of the pyrolyzed samples is sharper than the untreated biomass (raw rice husk and raw kenaf), which indicates that greater crystallinity occurs during the pyrolysis which is because of the polycrystalline structure that tends to depend on the cellulose content of the bioproduct.

The XRD results confirmed that rice husk biochar has a better crystallographic structure than kenaf biochar and that is due to the presence of  $\text{SiO}_2$  in the rice husk. Higher crystallinity results in reduced adsorption because it reduces the offset rate and therefore the alignment and should result in a “clean” surface with fewer parts and alternative defects. This is a high-energy site that is preferentially used for adsorption (Strnad et al. 2001).

### TGA analysis

TGA tests for rice husk and kenaf residues describe the thermal stability. The TGA curves of both types of biomass, in contrast with their biochar are shown in Figure 3. The most thermally stable Kenaf biochar, with minor decomposition events and maintaining the largest amount of carbonate residues, can be observed. On the other hand, the rice husk biochar lost about 35% of its density, while the raw rice husk was the least thermally stable, as it easily decomposed, leaving only 5% of its residual material. Over four consecutive steps, the two

**Table 2.** Ultimate analysis of raw materials and prepared pristine and blended biochar

Ultimate (wt.%)	Sample ratio Rice Husk: Kenaf					Sample ratio RHB: KFB				
	1.0:0	0.80:0.20	0.50:0.50	0.20:0.80	0.0:1.0	1.0:0	0.80:0.20	0.50:0.50	0.20:0.80	0.0:1.0
Carbon	37.8	38.1	38.5	39	39.2	56.4	55.3	52.75	47.9	46.7
Hydrogen	4.73	4.83	4.98	5	5.12	2.97	2.73	2.44	2.38	2.31
Nitrogen	0.45	0.57	0.67	0.85	0.98	0.26	0.35	0.43	0.46	1.2
Sulphur	0.91	0.66	0.56	0.38	0.22	0.3173	0.26	0.22	0.15	0.1133
Oxygen	42.9	43.5	44	44.9	45.6	40	48	50.3	55	56
O/C	1.15	1.141732	1.14	1.51	1.11	0.71	0.867993	0.95	1.15	1.2
H/C	0.125	0.13	0.13	0.12	0.13	0.053	0.05	0.075	0.05	0.05

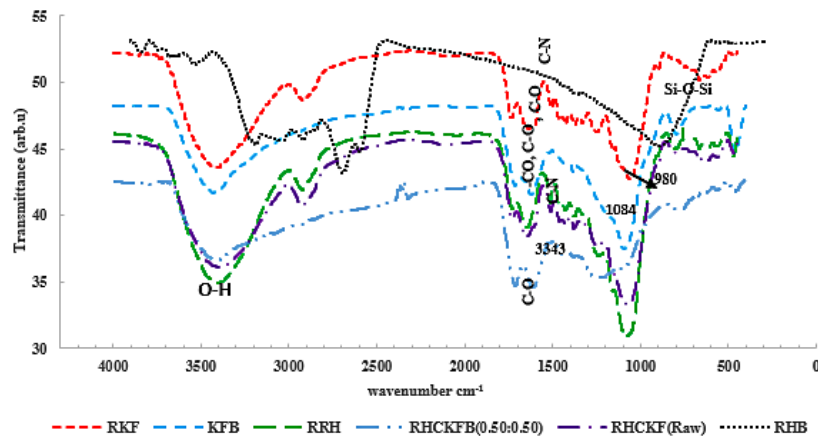


**Fig. 1.** Fourier transforms infrared (FTIR) spectra of raw rice husk (RRH), raw kenaf (RKF), rice husk biochar (RHB), kenaf fiber biochar (KFB), and composite biochar (RHCK).

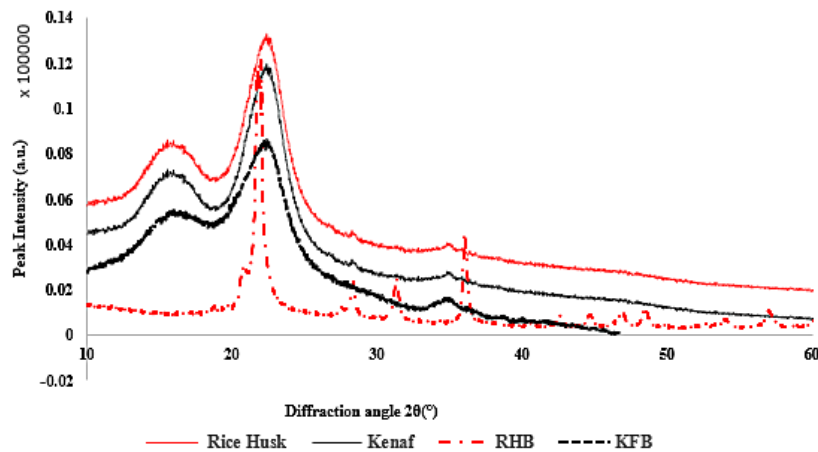


**Fig. 2.** XRD patterns of the biomass and biochar samples

types of biomass (rice husk and kenaf) display weight loss. The initial weight loss area between room temperature and 105 °C was identified in agricultural particles predominantly because of moisture-evaporation, hydroxyl water-soluble, and carboxyl groups contained in the particles. A breakup of glycoside connections and the thermal depolymerization of nanocellulose groups, such as hemicellulose and pectin are due to the sluggish degradation profile from 115 °C to 245 °C. The second deterioration collection occurred primarily between 240 °C and 310 °C, which implies weight loss due to the  $\alpha$ -cellulose decomposition. Around 290 °C to 460 °C was reached on the third shoulder peak, with the main peak of about 490 °C. In the fourth stage region, the degradation of the lignin content begins at 490 °C. The residual product decomposition shows a slow degradation profile above 550 °C. Kenaf has shown a 20% residual, while rice husk has shown a 5.5% and 5.92% residual.

The residual percentage of the particles represents the presence of ash and dust in the products of biomass.

### SEM micrograph

The pore characteristics of the different samples studied were analyzed using Scanning Electron Micrographs (SEM). As shown in Figure 4, the surface morphology changes in the biomass samples compared to their biochar due to the evaporation of biochar volatiles. The SEM images of rice husk biochar and kenaf biochar and rice husk blended kenaf biochar. Figures 4(d), (e), and (f) showed a great difference between the samples. In the SEM micrographs, the porous structures of each resulting biochar were shown, revealing a variety of types in the micropores, macropores, and mesopores.

The unpyrolyzed samples (rice husk and kenaf) were filled with tissue that was not

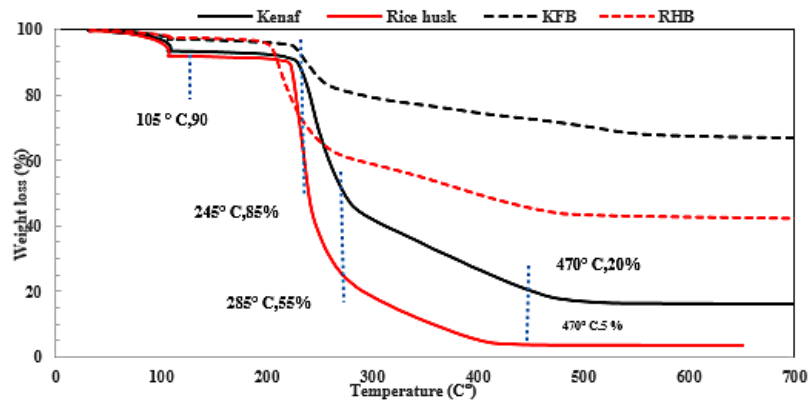


Fig. 3. TGA analysis of biomass and biochar

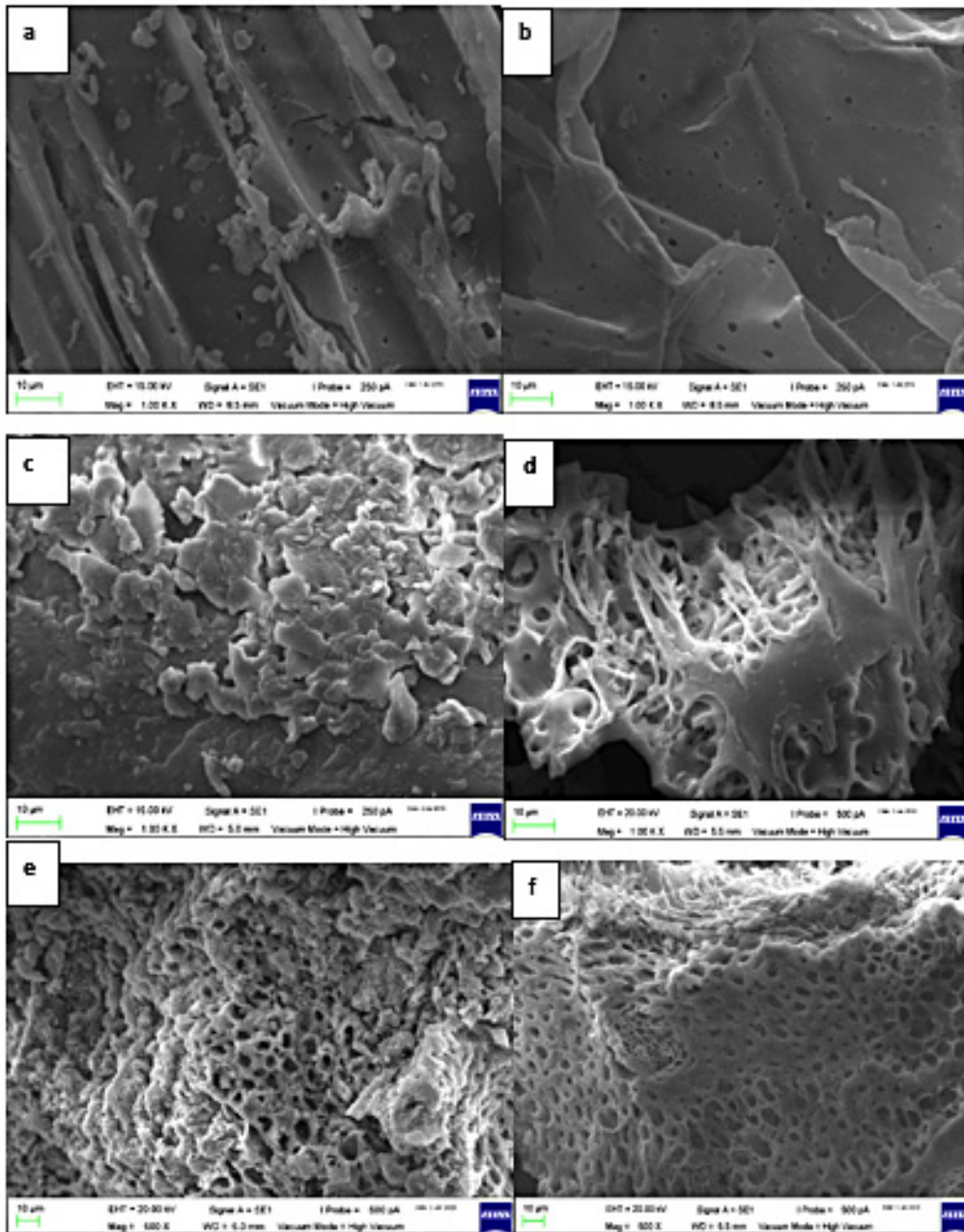


Fig. 4. SEM images of a) rice husk, b) kenaf, c) rice husk composite kenaf, d) rice husk biochar, e) kenaf biochar, and f) rice husk composite kenaf biochar

**Table 3.** SAP analysis of pristine and blended biochar and removal efficiency of Cu<sup>2+</sup>

BET	Sample ratio RHB: KFB				
	1.0:0	0.80:0.20	0.50:0.50	0.20:0.80	0.0:1.0
BET surface area (m <sup>2</sup> /g)	13.6	8.6	5.18	7.54	11.4
Pore volume (cm <sup>3</sup> /g)	0.0076	0.0079	0.0095	0.0032	0.017
Pore sizes (Å)	230	123	73.1	64.2	59.2
Removal efficiency of Cu <sup>2+</sup> (%)	65.80	45.50	21.60%	15.30	12.30

devolatilized; consequently, the pores were not fully developed. Nevertheless, the pyrolyzed samples which are pure rice husk biochar, kenaf biochar and composite biochar (RHB: KB,0.50:50) the morphology of the samples became honeycomb-like with cylindrical holes interconnected by some large holes but with different levels of porous structures.

### BET Characterization

Table 3 shows the analysis of BET surface area (m<sup>2</sup>/g), pore volume (cm<sup>3</sup>/g), pore size (Å), and removal efficiency of copper. The adsorption rate depends on the surface area of the adsorbent. When the surface area is large, the adsorbent can absorb more particles than the adsorbent with a small surface area. As shown in Table 3, the rice husk biochar relatively can absorb the copper ions from synthetic copper nitrate solution. The efficiency of pristine biochar compared to composite biochar based on the high specific surface area of pristine biochar indicated that the textural properties on biochar decrease as the blending ratio increases. The adsorbent that has a high surface area is better in terms of absorbing substances. Although the kenaf biochar adsorbent has high carbon atoms, rice husk biochar shows better adsorption efficiency of copper ions (Saeed, Harun, and Zulfani 2020). Composite biochar adsorption efficiency of copper ions increases along with the blending ratio of rice husk biochar to kenaf biochar (RHB: KB) increases as shown in Table 3, which proves that selection of raw materials biomass as a promising adsorbent is very important.

The copper ions interact with the biochar containing an extra ratio of rice husk due to high silica found in rice husk since rice husk constitutes siliceous aluminous material that sticks together and forms cementitious products when it reacts with water. Therefore, by adding rice husk biochar or rice husk ash it may become a medium to aid biochar in adsorbing heavy metal from aqueous solutions in wastewater.

### CONCLUSION

The rice husk biochar might be used as a blending material due to the high amount of silica. The BET result showed that a specific area of biochar decreases when there is blending or compositing of two biochar. The adsorption of copper ions increases when there is silica in biochar. The rice husk biochar showed good adsorption of copper ions from aqueous solutions. Blending does not give the desired result to be used as an adsorbent. The hypothesis was that the process of blending rice husk biochar with the kenaf biochar may improve the functional groups and aromatic character as well as the surface area/micropore volume of biochar. The hypothesis was also that the silica content found in rice husk may improve the adsorption, but characterizations completely denied the hypothesis. Biochar blending had a negative effect on the formation of biochar, as the ratio of oxygen to carbon and the ratio of hydrogen to carbon was outside the typical range which affects the biochar stability. Moreover, referring to Table 3, the effect of biochar blending negatively influenced the adsorption of copper ions from aqueous solutions.

### Acknowledgments

The authors would like to acknowledge the efforts of the Universiti Teknologi Petronas Malaysia for financing the project through Yayasan Universiti Teknologi PETRONAS with the grant code 015LC0-210.

### REFERENCES

- Ardejani F. D., Badii K., Limaee N. Y., Mahmoodi N. M., Arami M., Shafaei S. Z., and Mirhabibi A. R. 2007. Numerical modelling and laboratory studies on the removal of Direct Red 23 and Direct Red 80 dyes from textile effluents using orange peel, a low-cost adsorbent. *Dyes and Pigments*, 73(2), 178-185.

2. Chan K. Y., Van Zwieten L., Meszaros I., Downie A., and Joseph S. 2008. Agronomic values of green-waste biochar as a soil amendment. *Soil Research*, 45(8), 629-634.
3. Harun N.Y., Han, T.J., Vijayakumar T., Saeed A., and Afzal M.T. 2019. Ash Deposition Characteristics of Industrial Biomass Waste and Agricultural Residues. *Materials Today: Proceedings*, 19, 1712-1721.
4. Liu Z., and Zhang F.-S. 2009. Removal of lead from water using biochars prepared from hydrothermal liquefaction of biomass. *Journal of Hazardous Materials*, 167(1-3), 933-939.
5. Mubarak N. M., Kundu A., Sahu J. N., Abdullah E. C., and Jayakumar, N. S. 2014. Synthesis of palm oil empty fruit bunch magnetic pyrolytic char impregnating with FeCl<sub>3</sub> by microwave heating technique. *Biomass and Bioenergy*, 61, 265-275.
6. Renu, Agarwal, M., and Singh, K. 2017. Methodologies for removal of heavy metal ions from wastewater: an overview. *Interdisciplinary Environmental Review*, 18(2), 124-142.
7. Saeed A. A. H., Harun N. Y., and Nasef M. M. 2019. Physicochemical characterization of different agricultural residues in malaysia for bio char production. *International Journal of Civil Engineering and Technology (IJCIET)*, 10(10), 213-225.
8. Saeed A. A. H., Harun N. Y., and Zulfani N. 2020. Heavy Metals Capture from Water Sludge by Kenaf Fibre Activated Carbon in Batch Adsorption. *Journal of Ecological Engineering*, 21(6), 102-115.
9. Saeed A. A. H., Saimon N. N., Ali M. W., Kidam K., Jusoh Y. M., Jusoh M., and Zakaria Z. Y. 2018. Effect of Particle Size on the Explosive Characteristics of Grain (Wheat) Starch in a Closed Cylindrical Vessel. *Chemical Engineering Transactions*, 63, 571-576.
10. Saeed A. A. H., Sufian H.N.Y., Siyal S., Zulfiqar A.A., Bilad B., Vaganathan M.R., Al-Fakih A., Ghaleb A., Almahbashi A.A.S. 2020. Eucheuma cottonii Seaweed-Based Biochar for Adsorption of Methylene Blue Dye. *Sustainability* 12(24), 10318.
11. standards I. B. I. J. I. b. 2012. Standardized product definition and product testing guidelines for biochar that is used in soil.
12. Strnad S., Kreže T., Stana-Kleinschek K., and Ri-bitsch V. 2001. Correlation between structure and adsorption characteristics of oriented polymers. *Material Research Innovations*, 4(2-3), 197-203.
13. Tan X., Liu, Y., Zeng G., Wang X., Hu X., Gu Y., and Yang Z. 2015. Application of biochar for the removal of pollutants from aqueous solutions. *Chemosphere*, 125, 70-85.